

1 **TITLE:**

2 Quantification of Stokes drift as a mechanism for surface oil advection in the Gulf of Mexico

3

4 **AUTHORS:**

5 Matthew T. Clark<sup>1,2</sup>, Nicholas Heath<sup>1,2</sup>, Mark A. Bourassa<sup>1,2,3</sup>, and Eric P. Chassignet<sup>1,2</sup>

6

7

8 <sup>1</sup> Center for Ocean-Atmosphere Prediction Studies, Florida State University, Tallahassee, FL

9 32306-2741, USA.

10 <sup>2</sup> Department of Earth, Ocean, and Atmospheric Sciences, Florida State University, Tallahassee,

11 FL 32306-2741, USA.

12 <sup>3</sup> Geophysical Fluid Dynamics Institute, Florida State University, Tallahassee, FL 32306-2741,

13 USA

14

15 Corresponding author: . Mark A. Bourassa, Center for Ocean-Atmosphere Prediction Studies,

16 Florida State University, Tallahassee, FL 32306-2741, USA (mbourassa@coaps.fsu.edu)

17

18

19 Key points:

20 Surface water wave motion substantially contributes to transport of material transport at the

21 surface

22 Swell from tropical cyclones causes much greater transport

23 Waves have relatively greater impact in shelf waters

24

25

26	<b>INDEX TERMS AND KEYWORDS:</b>
27	4263 Ocean predictability and prediction
28	4255 Numerical modeling
29	4217 Coastal processes
30	4247 Marine meteorology
31	4251 Marine pollution
32	

33 **ABSTRACT:**

34 Wave-driven transport, also known as Stokes drift, is the motion of a particle due to the orbital  
35 motion induced by a passing wave. Stokes drift has previously been qualitatively shown to have  
36 a signature in ocean surface transport, with most studies focused exclusively in near-shore  
37 regions. However, Stokes drift has never been quantified beyond theoretical studies and case  
38 studies limited to small regions. Here, Stokes drift is calculated directly from Wavewatch III  
39 model data in the Gulf of Mexico for April-July 2010. Its magnitudes are compared between  
40 deep and shelf water areas, and against the magnitudes of surface currents and parameterized  
41 wind drift. These comparisons are also made specifically for the time period surrounding the  
42 passage of Hurricane Alex through the southwestern Gulf of Mexico. While there is not a major  
43 difference between the absolute magnitudes of Stokes drift in shelf vs. deep water areas or when  
44 compared to wind drift, Stokes drift is larger in shelf water areas relative to surface currents than  
45 in deep water. During Hurricane Alex, wave heights and there for Stokes drift magnitudes were  
46 much larger in the immediate area of the storm, which also led to much larger Stokes drift  
47 magnitudes in the oil spill region as the swell had propagated away from the storm and  
48 throughout the Gulf of Mexico.

49 **TEXT:**

## 50 **1. INTRODUCTION**

### 51 **1.1 Background**

52 On 20 April 2010, the *Deepwater Horizon* (DWH), a floating exploratory oil drilling  
53 platform, was drilling a well in the Gulf of Mexico at a depth of approximately 1,600 m when the  
54 well experienced a catastrophic blowout. That caused a large fire on the platform which led to  
55 the deaths of 11 workers, the sinking of the platform, and a leaking oil well on the ocean floor.  
56 From that moment until 15 July 2010, the well leaked approximately 58,000 barrels of oil per  
57 day into the Gulf [MacDonald 2010]. Some of this oil remained below the water surface, while  
58 the rest made it to the surface and was carried throughout the northeastern Gulf of Mexico.

59 First responders subsequently undertook efforts to prepare for and prevent the arrival of  
60 the oil to shorelines, through deployment of equipment such as booms and oil-collecting ships.

61 One element of these efforts was the use of oil spill forecast models to predict the future  
62 locations and tracks of the oil slicks, in order to more efficiently and effectively deploy those  
63 resources. These models typically incorporate weather and ocean current forecasts, and in some  
64 cases also lesser mechanisms such as wave- and wind-driven transport. For this study, we  
65 consider the effect of waves (known as Stokes drift) on the movement of oil in the Gulf of  
66 Mexico during the months in which the oil spill occurred.

### 67 **1.2 Stokes Drift**

68 Stokes drift is the lateral displacement of a particle in the direction of wave motion, due  
69 to the orbital motion of a passing wave train in a body of water. This effect was described by  
70 Stokes [1847] for finite-amplitude gravity waves. The displacement is due to the orbital motions  
71 not forming closed loops, which itself is due to the diminishing effects of horizontal

72 displacement with increasing depth. The forward motion of a particle on the surface at the crest  
73 of a wave (top of the orbit) is larger than the counter-motion backward at the trough of the wave  
74 (bottom of the orbit). The net displacement over a single wave period is the result of a second-  
75 order term in the overall wave motion equation, and so is sometimes disregarded in models.

76 There have been many studies in the past relating to the theoretical importance of Stokes  
77 drift to the overall transport of surface oil in the ocean. For example, Sobey and Barker [1997]  
78 used an idealized model of a near-shore region with along-shore current and onshore waves to  
79 determine the relative importance of Stokes drift. They found that Stokes drift was responsible  
80 for onshore beaching of surface oil in their model, in part due to the natural refracting of waves  
81 towards the shore by shoaling. Le Hénaff and Kourafalou [2012] found that including wind-  
82 induced drift (which includes Stokes drift) was beneficial to accurately modeling the movement  
83 of surface oil; hence we are interested in better quantifying contribution of Stokes drift.

84 Stokes' [1847] wave theory is predicated on the assumption of a homogeneous,  
85 incompressible fluid with uniform depth through which the wave is passing, and with the wave  
86 itself being of constant velocity and form throughout. For the consideration of determining  
87 Stokes drift velocities for a single ocean wave over a single wave period, these assumptions can  
88 be considered valid.

89 Stokes drift ( $U_s$ ) averaged over a single wave period is given by

$$90 \quad U_s = \frac{a^2 \sigma k \cosh(2k(H - z))}{2 \sinh^2(kH)} \quad (1)$$

91 where  $a$  is wave amplitude,  $k$  is the wave number,  $\sigma$  is the wave frequency,  $z$  is the depth being  
92 considered, and  $H$  is the depth of the water column on which the wave is occurring. Variables  
93 commonly found in wave models, however, include wave height ( $h$ ), wave period ( $T$ ), and  
94 wavelength ( $L$ ) [Monismith 2004]. Using the equations

95 
$$h = 2a , \tag{2}$$

96 
$$T = \frac{2\pi}{\sigma} , \tag{3}$$

97 and

98 
$$L = \frac{2\pi}{k} , \tag{4}$$

99 and assuming  $z = 0$  since for this study only Stokes drift at the surface is being considered,  
100 equation 1 becomes

101 
$$U_s = \frac{\pi^2 h^2}{LT} \frac{\cosh(2kH)}{2 \sinh^2(kH)} \tag{5}$$

102 This form of the equation accounts for both shallow and deep water waves. As waves move close  
103 to the coast the water becomes shallower, changing the wave characteristics relative to the deep  
104 water waves. The horizontal grid spacing of our ocean model limits the conditions to deep water  
105 in the vast majority of our cases; however we use the full equation to avoid artificial distinctions  
106 between shallow and deep water waves. Consequently there is little adjustment in wave direction  
107 and Stokes drift due to shoaling. Models that cover conditions closer to the coast would have to  
108 consider shoaling and its impact on wave transport. Le Hénaff and Kourafalou [2012] used a  
109 model in which Stokes drift was derived using two dimensional wave spectra. We tested both  
110 approaches in the Gulf of Mexico, and found that the results were practically identical. That  
111 assumption is expected to be valid in a semi-enclosed basin, but should not be used in a large  
112 ocean basin.

113 Stokes drift is often included in models via an approximation based on the wind speed  
114 and direction. This approximation includes surface motion due to Ekman transport, Stokes drift  
115 and directly wind forced drift, and the result is called “wind drift” [Weber 1983]. The common

116 range of values for this combined transport used in models is 2-5% of the 10 m wind speed at an  
117 angle  $20^\circ$  to the right of the wind direction [Hackett et al. 2006]. This approximation arose out  
118 of necessity, at a time when ocean and wave models were of insufficient resolution to allow for  
119 direct accounting of either Stokes drift or Ekman transport. However, this parameterization  
120 requires several assumptions, including wind wave equilibrium (that is, a steady sea state), and  
121 sufficient time for a full Ekman balance to develop, neither of which are reasonable in real-world  
122 conditions. Modern ocean models no longer require this approximation to be made, since Ekman  
123 transport can be more directly modeled. Additionally, modern wave models allow for Stokes  
124 drift to be calculated directly, which makes using a wind speed approximation for wind drift  
125 unnecessary and unreasonable (because it results in double the Ekman motion).

126         One reason for considering Stokes drift separately from using the wind speed-derived  
127 approximation is that Stokes drift can be present even without the presence of wind. Swell, by  
128 definition, is a wave that has propagated away from its area of formation. Stokes drift will be  
129 present for any wave, even swell, so therefore it will be present when swell is the only present  
130 portion of the wave spectrum. This is a situation that often occurs when there is calm, or with a  
131 very weak wind or recent wind such that the local wind wave field is not fully developed. Swell  
132 can also be present for higher local wind speeds if the swell waves are very large. A tropical  
133 cyclone is one example of a storm system that can create swell in the Gulf of Mexico.

134         Similarly, when considering oil as the material being transported, it is important to note  
135 the effect its presence on the ocean surface has on local waves. Oil has been observed and  
136 modeled to modify the wave field by damping out the shorter waves [Banger and Garrett 1968;  
137 Khalifa et al. 1992; Soloviev et al. 2011], reducing the surface roughness [Lindsley and Long  
138 2012], and hence increasing the wind speed [Zheng et al. 2013]. It also can reduce air-sea

139 friction, further inhibiting local wave development. However, this impact is minimized on swell  
140 originating away from an oil slick, which results in the presence of the Stokes drift factor in  
141 regions affected by an oil spill. Additionally, when high wind speeds occur over an oil slick, the  
142 slick tends to break apart, reducing this effect, both through turbulence in the upper ocean layer  
143 and wave breaking, mixing oil into the water column. However, wind speeds of sufficient  
144 magnitude to do this are not commonplace in the Gulf of Mexico except in tropical cyclones and  
145 winter cold frontal passages.

146         Basing Stokes drift calculation on wind speed at a given level also ignores the different  
147 manners in which the wind can interact with the ocean surface, and thus how the sea state will  
148 develop given a particular (e.g. 10 m) wind speed. A wind profile in a stable atmospheric  
149 surface layer (which occurs frequently at night) will result in weaker wind stress at the  
150 atmosphere/water boundary, leading to smaller waves. Conversely, an unstable atmospheric  
151 surface layer, even with the same 10 m wind speed, will result in greater wind stress at the  
152 atmosphere/water boundary, leading to larger wave heights and thus larger Stokes drift  
153 magnitudes for the same wind speed at the given height. Additionally, drift is affected by  
154 whitecapping and wave breaking, which violate the assumptions listed above. In the Gulf of  
155 Mexico, winds are usually light enough that Stokes drift is a valid approximation.

### 156 **1.3 Outline**

157         This study quantifies the effect of Stokes drift on the transport of surface oil in the Gulf  
158 of Mexico during the DWH spill. The data used in the study as well as the methods by which  
159 Stokes drift is determined from that data is presented (Chapter 2). The results of the calculation  
160 of Stokes drift in the Gulf of Mexico during the months of the oil spill are given. 24-hour  
161 displacements due to Stokes drift are also examined, as well as comparisons to surface ocean

162 currents and wind drift (Chapter 3). The impact of a hurricane which occurred during the study  
163 period are detailed (Chapter 4). It will be shown that Stokes drift was an important factor in the  
164 transport of oil during the DWH spill, and thus it is important to accurately account for Stokes  
165 drift in models.

166

167

## 2. DATA AND METHODS

168

### 2.1 Wavewatch III

169

170

171

172

173

174

175

#### 2.1.1 Existing Data

176

177

178

179

180

181

182

183

184

An existing dataset was considered. The U.S. National Center for Environmental Prediction (NCEP) offers model hindcasts globally from the present time back to 1997, at three-hour intervals [NOAA 2009]. These wave hindcasts are forced by Global Forecast System (GFS) wind input. However, this data was incomplete in the Gulf of Mexico, as the gridded peak wave period output contained spatial gaps for undetermined reasons (Figure 1). In addition, the highest-resolution output available ( $1/15^\circ$  grid) is only available for regions within approximately 100 km of coasts. More coarse data ( $1/6^\circ$ ) was available covering the entire Gulf, but that also contained the peak period gaps. So, in order to acquire a full, complete gridded dataset to cover the study period of April-July 2010, it became necessary to use a wave model to

185 create high-resolution continuous wave data for the entire Gulf specifically to be used for this  
186 study. Accordingly, the Wavewatch III model was utilized.

### 187 **2.1.2 Running Wavewatch III**

188 Wavewatch III [Tolman 2009] is a spectral wind wave model that can simulate wind-  
189 generated local wave fields and swell propagating from non-local areas. It was developed by the  
190 Marine Modeling and Analysis branch of the Environmental Modeling Center, within NCEP.  
191 Wavewatch works by separating wave spectrum at each grid point into partitions by energy  
192 density peaks, as well as calculating peak and mean wave variables for the entire spectrum. The  
193 model has available a number of parameterization and other options. Wavewatch can also accept  
194 several input parameters as wave forcing and limiting mechanisms, including near-surface  
195 atmospheric winds, sea ice concentrations, and air and sea-surface temperatures. For this work,  
196 ice is not included (since the area of interest is the Gulf of Mexico, where ice is not present).  
197 Atmospheric wind and temperature and sea-surface temperature are included, in order to allow  
198 for surface stress adjustment due to stability.

199 The model was set up with a  $1/15^\circ$  grid covering the Gulf of Mexico ( $18-31^\circ$  N,  $80-100^\circ$   
200 W) with a time step of 450 seconds, nested within a coarser grid ( $1/2^\circ$  spacing) covering all of  
201 the north Atlantic Ocean ( $5^\circ$  S- $55^\circ$  N,  $5-100^\circ$  W) with a time step of 900 seconds (Figure 2).  
202 Boundary conditions for the coarse grid (except for the western boundary, which is entirely land)  
203 and the initialization of both grids were done using the idealized Joint North Sea Wave  
204 Observation Project (JONSWAP) spectrum [Hasselmann 1973]. This initialization was done to  
205 provide a starting point, after which the model was run for a two-week period (prior to the  
206 beginning of the study period) using model data (see below) for forcing, ensuring that any  
207 spurious wave energy in the model should be dissipated before analysis data was generated,

208 leaving only waves driven by actual wind. Similarly, by placing the coarse grid boundaries a  
209 considerable distance from the fine grid boundaries (which received boundary conditions from  
210 the coarse grid), JONSWAP-influenced wave energy was dissipated before it propagated into the  
211 fine grid.

212         Although the period of interest for this work is April-July 2010, Wavewatch was  
213 initialized at 15 March 2010 00Z, and run through 10 August 2010 00Z. The early start was  
214 intended to provide a "spin-up" of the model to reduce spurious world-driven wave energy from  
215 the JONSWAP initialization. The extended run time allowed for sufficient additional data to be  
216 generated to calculate trajectories initialized as late as July 31.

217         Wavewatch was forced using both atmospheric wind and temperature and sea-surface  
218 temperature (SST). Using both temperatures is important, as doing so provides the model with  
219 the ability to approximate the wind profile between the height of the "measurement" wind and  
220 the surface. Forcing data for this work was obtained from NCEP's Climate Forecast System  
221 Reanalysis (CFSR) [Saha 2010]. This product originally existed only for the period from 1979-  
222 2009, but was recently extended through 2010. Atmospheric wind was taken from the 10 m  
223 wind velocities. Temperatures were used from the water surface and from a height of 2 m.  
224 Water depths were provided by NOAA's World Geophysical Data Center 2-minute Gridded  
225 Global Relief Data (ETOPO2v2) [NGDC 2001]. It should be cautioned that this implementation  
226 of Wavewatch III does not include the effects of currents, which would affect the wind stress  
227 levels at the air-sea boundary (by changing the wind velocity relative to a particular point on the  
228 surface, which would then be initially moving with the current rather than only with the wave  
229 motion).

230 The model was set to save output data at each hour. Three output variables were used for  
231 this work: significant wave height ( $h$ ), peak wave period ( $T$ ), and peak wave direction ( $\theta$ ).  
232 Notably, the peak period output did not contain the gaps present in the already-existing data  
233 (Figure 3). All were chosen as they are commonly available in both observations and models,  
234 and can be used to calculate Stokes drift. Wavelength ( $L$ ) was then calculated from the peak  
235 period ( $T$ ), using the deep-water wavelength

$$L_0 = \frac{gT^2}{2\pi} \quad (6)$$

237 and the dispersion relation

$$L = L_0 \tanh\left(\frac{2\pi H}{L}\right) \quad (7)$$

239 to reach a final wavelength for use in Eq.(5). Stokes drift was then calculated at each point in the  
240 Gulf of Mexico at each hourly time step from 1 April 2010 00Z to 10 August 2010 00Z.

## 241 2.2 Methods

### 242 2.2.1 Stokes Drift

243 In order to provide a basic overview of Stokes drift in the Gulf of Mexico, Stokes drift  
244 was calculated using Eq.(5) at each point in the model domain, restricted to the Gulf (meaning,  
245 excluding the portions of the Caribbean Sea and Atlantic Ocean present in the model domain) at  
246 each hourly time step from 01 April 2010 00Z to 31 July 2010 23Z, so as to include the time  
247 period of and some time before and after the spill. Any points for which any data needed for  
248 calculating Stokes drift (wave height, period, length, or direction) were missing were excluded,  
249 which occurred 0.08% of the time. Additionally, grid points at which the water depth was less  
250 than 1 m were also excluded, since these locations were so near to land that waves are either  
251 breaking or likely directed onshore.

252           It is also useful to consider Stokes drift as a comparison between deep water and shelf  
253 water areas. Water waves in sufficiently shallow water (how shallow is dependent on  
254 wavelength) interact with the ocean bottom, resulting in changes to wave parameters such as  
255 height and speed that are included in the calculation of Stokes drift. Additionally, shelf water  
256 does not have the large (and deep) eddies of the open Gulf, but does have substantial coastal  
257 currents; therefore there could be a different distribution of surface velocities (which we will  
258 refer to as currents). Therefore, we examine the relative importance of Stokes drift and currents  
259 in the deep Gulf and on the shelves. For this study, the boundary between shallow/shelf and  
260 deep water is set at 100 meters. This provides for the approximate separation of the shallow  
261 continental shelf areas from the deep ocean.

### 262 **2.2.2 Trajectories**

263           Another method of comparing Stokes drift between deep and shelf water is with the use  
264 of trajectories. This allows for considering not how Stokes drift magnitudes change at a point,  
265 but instead considering what would happen to a theoretical particle (such as a patch of oil  
266 floating on the surface) over time due to Stokes drift. Here, with Stokes drift velocities  
267 calculated at each grid point every hour, it is possible to consider the net displacement of a  
268 particle over a period of time (here chosen to be 24 hours) due solely to Stokes drift. Particles  
269 are considered massless and infinitely small, which means they offer no resistance to their  
270 theoretical movement. In order to determine net displacements, at each hour in the data, a tracer  
271 grid was initialized at each velocity grid point in the Gulf of Mexico. For each of 24 successive  
272 hours, a new position was calculated for each position grid point based on the Stokes drift  
273 velocity field for that hour, and except for the initial advection (when all grid points were co-  
274 located with the initial velocity grid points), the velocity applied according to a Runge-Kutta

275 interpolation of that hour's Stokes drift velocity field. If a position grid point was at any time  
276 advected off the velocity field, it was considered stopped at its last known point for the  
277 remainder of the time. Once the tracer points had been advected for 24 hours, the distance they  
278 had ended up from their initial locations was then calculated.

### 279 **2.2.3 Stokes Drift and Other Transport Mechanisms**

280 Stokes drift is, of course, not the only transport mechanism that contributes to the  
281 movement of surface oil. For this study, Stokes drift is compared to modeled surface currents  
282 the data-assimilative Gulf of Mexico (GOM) HYCOM experiment\_31.0 and compared to wind  
283 drift (see section 1.2 for details) as 2% of the CFSR 10 m wind speed at a declination of 20°.  
284 The HYCOM model data is on a 1/25° spatial and 1-hour temporal grid, and does not include tidal  
285 forcing. The CFSR model data is on a 1/3° spatial and 1-hour temporal grid. Both products are  
286 hindcasts and were interpolated onto the 1/15° grid used by Wavewatch. Both HYCOM and CFSR  
287 are data-assimilative, meaning that they should be reasonably robust for this purpose. For both  
288 comparisons, magnitude of the Stokes drift is divided by the magnitude of the alternative surface  
289 transport mechanism to produce a ratio at each grid point and time. These ratios are then  
290 compared between deep and shelf water areas.

291 The data-assimilative GOM HYCOM experiment\_31.0 has a ~4 km (1/25°) horizontal grid  
292 spacing at the latitude of the GOM and uses 20 vertical coordinate surfaces. The model uses a  
293 hybrid vertical layering system, employing isopycnal layers in the stratified open ocean, terrain-  
294 following coordinates in coastal areas, and fixed pressure-coordinates in the mixed layer [Bleck,  
295 2002; Chassignet et al., 2006]. Interface depths change at each time step to reflect thermohaline  
296 variability, and layers are more closely spaced in the upper ocean. Outputs are interpolated to a  
297 nominal latitude-longitude-depth grid and archived in NetCDF format. The model is run in near  
298 real time at the NAVOCEANO Major Shared Resource Center to produce seven-day forecasts

299 and four-day hindcasts. Hourly hindcast data are publicly available on the HYCOM consortium  
300 data server (<http://hycom.org/dataserver>). HYCOM 31.0 uses the 3D-VAR Navy Coupled Ocean  
301 Data Assimilation (NCODA) system [Cummings, 2005; Cummings and Smedstad, 2013].  
302 NCODA assimilates all available observations. These include surface information from satellites  
303 (SST and SSH), plus in situ temperature and salinity profiles from XBTs (expendable  
304 bathythermographs), CTDs (conductivity-temperature-depth), gliders, and Argo floats  
305 [Chassignet et al., 2007, 2009; Cummings and Smedstad, 2013; Metzger et al., 2014]. Satellite  
306 altimetry for NCODA comes from the NAVOCEANO Altimeter Data Fusion Center, which  
307 combines SSH from Jason-1, OSTM/Jason-2, Geosat, and Envisat. Vertical projection of the  
308 surface observations is achieved via generation of synthetic profiles using the Modular Ocean  
309 Data Analysis System [MODAS; Fox et al. 2002]. For a detailed description of the model and its  
310 outputs, the reader is referred to <http://hycom.org/data/goml0pt04/expt-31pt0> and to Rosburg et  
311 al. [2016]. For a detailed description of HYCOM, the reader is referred to Bleck [2002],  
312 Chassignet et al. [2003], and Chassignet et al. [2006].

### 313 **3. STOKES DRIFT IN THE GULF OF MEXICO**

#### 314 **3.1 Stokes Drift in the Full Gulf of Mexico**

315 For the Gulf of Mexico as a whole, the average Stokes drift magnitude was 3.99 km/day,  
316 while the median was 3.40 km/day (see Table 1) during the study period. This indicates that the  
317 distribution of Stokes drift magnitudes skewed towards smaller values (in fact, this is the case for  
318 all Gulf-wide Stokes drift-related distributions considered in this study) (Figure 4). In addition,  
319 there was a wide variation in the distribution of wave (and therefore Stokes drift) directions,  
320 although the vast majority of waves during the period did have at least some westward  
321 component (Figure 5).

322

### 3.2 Stokes Drift Comparison - Deep vs. Shelf Water

323

324

325

326

327

328

329

For waves occurring over shelf water, Stokes drift magnitudes averaged 3.70 km/day with a median of 3.09 km/day, while for deep water Stokes drift magnitudes averaged 4.12 km/day with a median of 3.52 km/day (Table 2). In addition, magnitudes in shelf water exhibited a smaller variation, with a standard deviation of 2.78 vs. 2.91 km/day in deep water (Figures 6) It is unclear whether the larger average Stokes drift magnitudes in deep water are simply the result of larger waves due to higher wind speeds, or to what extent, if any the slowing of waves due to bottom interaction was responsible.

330

331

332

333

334

335

336

337

338

The small difference between the average Stokes drift magnitudes for deep and shelf water is not unexpected. While conventional wisdom does hold that “shallow water” waves generally have larger Stokes drift magnitudes, this is in reference to shallow water waves which are interacting with the ocean bottom. This is not the comparison being made here. The large majority of waves occurring over shelf water (again, defined for this study as depths of 100 m or less) are in fact still deep-water waves by that definition. Waves in the Gulf of Mexico are rarely large enough to become “shallow water” waves except in very shallow water (for example, depths of less than 10 m), which in this study constitutes a very small number of grid points.

### 3.3 Stokes Drift Compared to Current and Wind Drift

339

340

341

342

343

344

While Stokes drift showed a small difference when comparing deep and shelf water areas, this difference is much more pronounced when comparing Stokes drift magnitudes to surface current magnitudes. In deep water areas, Stokes drift magnitudes were an average of 20.8% of the collocated surface current (Figure 7). However, in shelf water areas, Stokes drift was 36.0% of the surface current magnitude on average, with a much wider distribution of ratios (Figure 10). This means that Stokes drift is a more significant relative factor in surface transport

345 in shelf water areas, and so accurate representation of Stokes drift in transport models is more  
346 important in these areas.

347 Stokes drift is a larger contribution to the total surface transport of oil in shelf water  
348 primarily due to these areas having smaller surface current magnitudes. As seen previously,  
349 there is not a large difference in Stokes drift magnitudes themselves between deep and shelf  
350 water, while large magnitudes of surface current are primarily found in the loop current and loop  
351 current eddies, which are largely confined to deep water areas.

352 Similar comparisons were made with Stokes drift and a percentage of the wind speed  
353 ("wind drift"). Here, 2% of the wind speed is considered, which is at the bottom of the range of  
354 wind drift parameterizations used in trajectory models. As shown in Figures 8, there is little  
355 difference in ratios when comparing between deep and shelf water areas (which is expected since  
356 both regions typically experience similar wind speeds). However, it *can* be seen that there is a  
357 wide distribution of ratios of Stokes drift to 2% of the wind speed in both figures. This indicates  
358 that there is poor correlation of Stokes drift and wind speed, implying that using wind speed as a  
359 proxy for Stokes drift is not especially accurate. Since there is sometimes swell propagating into  
360 a region from elsewhere, and sea state does not instantaneously change in response to changing  
361 wind speeds, this is not an unexpected result, however the example of the magnitude of the error  
362 highlights the importance of using more physically sound approaches to modeling surface  
363 transport.

364

#### 365 **4. STOKES DRIFT DURING A HURRICANE**

366 While Stokes drift is induced by any wave, the largest magnitudes of Stokes drift are  
367 generally produced by the largest waves. Correspondingly, the largest waves in the Gulf of

368 Mexico are produced by the strongest winds, which are almost always found in tropical cyclones.  
369 In addition, large waves produced by these storms propagate away to become significant swell in  
370 locations within the Gulf well away from their origins. This produces an extreme case in which  
371 Stokes drift as estimated from the local wind speed can be especially inadequate as a means of  
372 accounting for particle displacement.

373 During the four months of this study, two tropical cyclones passed through the Gulf of  
374 Mexico. Hurricane Alex occurred in late June, while Tropical Depression Bonnie (previously a  
375 tropical storm) occurred in late July. Bonnie was not considered for this study, due to being  
376 below tropical storm-force for its entire presence in the Gulf.

#### 377 **4.1 Hurricane Alex**

378 Hurricane Alex formed in the Caribbean Sea on June 24, 2010 as a tropical depression,  
379 then strengthened into a tropical storm, crossing the Yucatan Peninsula and entering the  
380 southwestern Gulf of Mexico on June 27 with maximum sustained wind speeds of 35 kt. The  
381 storm then moved northwest across the western Gulf, strengthening into a category 2 hurricane  
382 with maximum sustained wind speeds of 95 kt, before making a second landfall on the northern  
383 Mexico coast on July 1 [Pasch 2010]. This resulted in a period of approximately 72 h during  
384 which large-height waves were being generated by increasingly strong winds across the  
385 southwestern Gulf of Mexico. These waves were of sufficient size and energy that they could  
386 propagate throughout the Gulf of Mexico as swell before dissipation.

387 To examine how Hurricane Alex affected Stokes drift magnitudes across the Gulf, two  
388 regions within the Gulf are compared before, during, and after the storm. The first of these  
389 regions is the southwestern Gulf, where the storm had a direct impact on wave heights, while the  
390 second region is the northeastern Gulf, where the oil spill was occurring and distant from the

391 hurricane's winds (Figure 9). For each region, Stokes drift magnitudes are compared during  
392 three seven-day periods: one before the storm entered the Gulf, one encompassing the entire  
393 time any part of the storm's circulation was over the Gulf, and one following the storm's landfall  
394 (see Table 3). Seven-day periods are intended to be short enough to prevent the effects of the  
395 hurricane on Stokes drift from being lost as noise, while being long enough to not be affected by  
396 daily and day-to-day random weather events.

#### 397 **4.2 Stokes Drift During Hurricane Alex**

398 During the week before Alex entered the Gulf of Mexico, Stokes drift magnitudes in the  
399 southwestern Gulf study region averaged 2.69 km/day, which was below the region's four-month  
400 average of 3.03 km/day, with a standard deviation of 1.47 (Figure 10 red line, and Table 4).  
401 Similarly, Stokes drift magnitudes in the northeastern Gulf averaged 1.89 km/day with a standard  
402 deviation of 1.82, which was also below that region's four-month average of 3.22 km/day (Figure  
403 11, red line, and Table 5). As Alex traversed the southwestern Gulf of Mexico, its winds  
404 generated large waves. This resulted in that week's average Stokes drift magnitude in the region  
405 rising sharply to 7.64 km/day, which lies at the 88th percentile of the four-month period (Figure  
406 10, blue line, and Table 4). The distribution of magnitudes during that time period also increased  
407 drastically, with the standard deviation rising to 5.16. In the northeastern Gulf, the mean Stokes  
408 drift magnitude also rose, but only to 2.82 km/day, which was still below the area's four-month  
409 average. However, the variability of the magnitudes also increased to 2.41 (Figure 11, blue line,  
410 and Table 5). It is likely that most (but not all) of the storm-produced wave energy during this  
411 period was still remaining in the southwestern Gulf, with only a small amount having propagated  
412 away into the northeastern Gulf to boost Stokes drift values there.



436 period of time, the basic principle, that Stokes drift is an important surface transport mechanism  
437 and should be accounted for in models in the most precise manner available, is logically  
438 applicable for any body of water on which wind waves form.

439         When comparing Stokes drift for waves occurring in water of relatively shallow depth  
440 (the continental shelf, delineated as water of depth less than 100 m) against that for waves  
441 occurring in deeper water (depth greater than or equal to 100 m), no physically significant  
442 difference in magnitude was found during the study period. This is most likely because waves  
443 are primarily wind-driven, and there was little if any difference in wind speeds over waters of  
444 differing depths. It is possible that for areas of sufficiently shallow depth that waves interact  
445 with the ocean bottom, there may have been a more notable difference, but the Gulf of Mexico  
446 has relatively small waves when compared with other basins, due to lighter winds and scarcity of  
447 swell, especially during the spring and summer months included in this study. This means that  
448 the number of grid points and times wherein waves would be impacted by bottom interaction  
449 was small.

450         However, when comparing Stokes drift magnitudes to surface current magnitudes, there  
451 is a notable difference between shelf and deep water. Stokes drift is a larger relative component  
452 in overall surface transport compared to surface current in shelf water, approximately double the  
453 percentage of the local current magnitude, when compared to deep water. This is primarily due  
454 to weaker surface currents in shallower water. Therefore, if calculating Stokes drift in an oil spill  
455 model with limited computing resources, it is more important to do so for shallow/shelf water  
456 areas, as Stokes drift is a larger part of total surface transport there.

457         While Stokes drift is often approximated in surface transport models as a percentage of  
458 the wind speed at a specific angle from the wind direction, it is not the best way to account for

459 Stokes drift if the model includes a wave component. This is because Stokes drift has significant  
460 variation from the wind, due to the lag between changing wind speed and sea state response, as  
461 well as swell propagating into a region from elsewhere. This means that there are often waves  
462 (and with them, Stokes drift) occurring even when the local wind is calm. Thus, when designing  
463 a trajectory model which includes waves, it is preferable to calculate the Stokes drift component  
464 of transport directly from the wave parameters rather than using the wind speed approximation.

465         During weather events that involve high wind speeds over long time periods and large  
466 areas, such as hurricanes, waves (and with them, Stokes drift magnitudes) can grow very large.  
467 Swell propagating out from these areas into more distant areas can make a wind speed  
468 approximation of Stokes drift especially inaccurate. Additionally, Stokes drift can become a  
469 much more significant fraction of the total surface transport. This effect can last for a few days  
470 after the storm has exited the basin, indicating that Stokes drift due to swell is an important  
471 consideration and that wave models should be used when estimating surface transport.

472

473 Acknowledgements: This research was made possible in part by a grant from The Gulf of  
474 Mexico Research Initiative, and in part by Bureau of Ocean Energy Management WAMOST  
475 project (M12PC00003), NASA PO and NOAA/COD. Data are publicly available through the  
476 Gulf of Mexico Research Initiative Information & Data Cooperative (GRIIDC) at  
477 <https://data.gulfresearchinitiative.org> (doi:<doi identifier>).

478

479

480 **REFERENCES:**

481 Banger, W. R. and W. D. Garrett (1968) Modification of the air/sea interface by artificial sea  
482 slicks, NRL Report 6762, Naval Research Laboratory, 18pp.

483 Bleck, R., 2002. An oceanic general circulation model framed in hybrid isopycnic-  
484 Cartesian coordinates. *Ocean Modelling* 4 (1), 55-88.

485 Chassignet, E. P., Smith, L. T., Halliwell, G. R., Bleck, R., 2003. North Atlantic simulation  
486 with the HYbrid Coordinate Ocean Model (HYCOM): Impact of the vertical  
487 coordinate choice, reference density, and thermobaricity. *J. of Phys. Oceanogr.* 33,  
488 2504-2526.

489 Chassignet, E. P., Hurlburt, H. E., Smedstad, O. M., Halliwell, G. R., Walcraft, A. J., Metzger,  
490 E. J., Blanton, B. O., Lozano, C., Rao, D. B., Hogan, P. J., Srinivasan, A., 2006.  
491 Generalized vertical coordinates for eddy-resolving global and coastal ocean forecasts.  
492 *Oceanography* 19, 20-31.

493 Chassignet, E. P., H. E. Hurlburt, O. M. Smedstad, G. R. Halliwell, P. J. Hogan, A. J. Wallcraft,  
494 R. Baraille, and R. Bleck (2007), The HYCOM (HYbrid Coordinate Ocean Model) data  
495 assimilative system, *J. Mar. Syst.*, 65, 60–83, doi:10.1016/j.jmarsys.2005.09.016

496 Chassignet, E., Hurlburt, H., Metzger, E. J., Smedstad, O., Cummings, J., Halliwell, G., Bleck,  
497 R., Baraille, R., Wallcraft, A., Lozano, C., Tolman, H., Srinivasan, A., Hankin, S.,  
498 Cornillon, P., Weisberg, R., Barth, A., He, R., Werner, F., Wilkin, J., 2009. US GODAE:  
499 Global Ocean Prediction with the HYbrid Coordinate Ocean Model (HYCOM).  
500 *Oceanography* 22 (2), 64-75.

501 Cummings, J. A., 2005. Operational multivariate ocean data assimilation. *Q. J. Roy. Meteor.*  
502 *Soc.* 131 (613), 3583-3604.

503 Cummings, J. A., Smedstad, O. M., 2013. Variational data assimilation for the global ocean. In:  
504 Park, S. K., Xu, L. (Eds.), Data Assimilation for Atmospheric, Oceanic and Hydrologic  
505 Applications (Vol. II). Springer Berlin Heidelberg, pp. 303-343.

506 Fox, D., Teague, W., Barron, C., Carnes, M., Lee, C., 2002. The Modular Ocean Data Analysis  
507 System (MODAS). *J. Atmos. Ocean Tech.* 19, 240-786.

508 Hasselmann, K., *et al.* (1973), Measurements of wind-wave growth and swell decay during the  
509 Joint North Sea Wave Project (JONSWAP), *Dtsch. Hydrogr. Z. Suppl.*, 12A8, 1–95.

510 Khalifa, S. S., B. Linde, S. Pogorzelski, and A. Śliwiński (1992). The attenuation of short surface  
511 wind waves by monolayer oil films, *Oceanologia*, 32, 41-47.

512 Le Hénaff, M., V. H. Kourafalou, C. B. Paris, J. Helgers, Z. M. Aman, P. J. Hogan, and A.  
513 Srinivasan (2012), Surface Evolution of the Deepwater Horizon Oil Spill Patch:  
514 Combined Effects of Circulation and Wind-Induced Drift, *Environmental science &*  
515 *technology*, 46.13, 7267-7273, doi:10.1021/es301570w

516 Lindsley, R.D. and D.G. Long (2012), Mapping Surface Oil Extent From the Deepwater Horizon  
517 Oil Spill Using ASCAT Backscatter. *IEEE Trans. Geosci. Remote Sensing*, 50(7), 2534–  
518 2541, doi:10.1109/TGRS.2011.2174369.

519 Liu, Y., R.H. Weisberg, C. Hu, and L. Zheng (2011), Tracking the Deepwater Horizon oil spill:  
520 A modeling perspective, *Eos, Trans. Amer. Geophys. Union.*, 92, 45–46,  
521 doi:10.1029/2011EO060001

522 MacDonald, I. (2010): Deepwater disaster: How the oil spill estimates got it wrong,  
523 *Significance*, 7(4), 149–154, doi:10.1111/j.1740-9713.2010.00449.x

524 Metzger, E. J., Smedstad, O. M., Thoppil, P. G., Hurlburt, H. E., Cummings, J. A., Wallcraft, A.  
525 J., Zamudio, L., Franklin, D. S., Posey, P. G., Phelps, M. W., Hogan, P. J., L., B. F.,

526 DeHaan, C. J., 2014. US Navy operational global ocean and Arctic ice prediction  
527 systems. *Oceanography* 27 (3), 32-43.

528 Monismith, S., and D. Fong (2004), A note on the potential transport of scalars and organisms by  
529 surface waves, *Limnology and Oceanography*, 49, 1214-1217,  
530 doi:10.4319/lo.2004.49.4.1214

531 NGDC (National Geophysical Data Center/NESDIS/NOAA/U.S. Department of Commerce)  
532 (2001), ETOPO2, Global 2 Arc-minute Ocean Depth and Land Elevation from the US  
533 National Geophysical Data Center (NGDC), Research Data Archive at the National  
534 Center for Atmospheric Research, Computational and Information Systems Laboratory,  
535 Boulder, Colo. Accessed 6 June 2013.

536 NOAA, cited 2009: NWW3 implementations. [Available online at  
537 <http://polar.ncep.noaa.gov/waves/implementations.shtml>].

538 Pasch, R., 2010.: Tropical Cyclone Report: Hurricane Alex (AL012010) 25 June – 2 July 2010,  
539 NOAA/National Weather Service, Miami, Fla.

540 Rosburg, K.C., K.A. Donohue, and E.P. Chassignet, 2016. [Three-dimensional model-observation](#)  
541 [intercomparison in the Loop Current region](#). *Dyn. Atmos. Oceans*, in press.

542 Saha, S., et al. (2010), NCEP Climate Forecast System Reanalysis (CFSR) Selected Hourly  
543 Time-Series Products, January 1979 to December 2010, Research Data Archive at the  
544 National Center for Atmospheric Research, Computational and Information Systems  
545 Laboratory, Boulder, Colo., <http://dx.doi.org/10.5065/D6513W89>, Accessed 20 Sep  
546 2013.

547 Sobey, R.J., and C.H. Barker (1997), Wave-driven transport of surface oil, *J. Coas. Res.*, 13,  
548 490–496.

549 Soloviev, A., S. Matt, M. Gilman, H. Hühnerfuss, B. Haus, D. Jeong, I. Savelyev,  
550 M. Donelan, 2011: Modification of turbulence at the air-sea interface due to the presence  
551 of surfactants and implications for gas exchange. Part I: laboratory experiment. In: *Gas*  
552 *Transfer at Water Surfaces*, Kyoto University Press, 245 – 258.

553 Stokes, G. G., 1847), On the theory of oscillatory waves, *Trans. Cambridge Phil. Soc.*, 8, 441–  
554 455.

555 Tolman, H. (2009), User manual and system documentation of WAVEWATCH III TM version  
556 3.14, Technical note, MMAB Contribution 276.

557 Weber, J. (1983), Steady wind-and wave-induced currents in the open ocean, *J. Phys. Oceanogr.*,  
558 13.3, 524-530, doi:10.1175/1520-0485(1983)013<0524:SWAWIC>2.0.CO;2

559 Zheng, Y., M. A. Bourassa, and P. J. Hughes (2013), Influences of Sea Surface Temperature  
560 Gradients and Surface Roughness Changes on the Motion of Surface Oil: A Simple  
561 Idealized Study. *J. Appl. Meteor. Clim.*, doi:10.1175/JAMC-D-12-0211.1.

562 **TABLES:**

563 Table 1: Stokes drift magnitudes, full Gulf of Mexico, April-July 2010

<b>Parameter</b>	<b>Value (km/day)</b>
Mean	3.99
9th percentile	0.76
25th percentile	1.79
Median (50th percentile)	3.40
75th percentile	5.63
91st percentile	8.13
Standard deviation	2.88

564

565

566 Table 2: Stokes drift magnitudes, deep vs. shelf water, Gulf of Mexico, April-July 2010

<b>Parameter</b>	<b>Deep Water Value (km/day)</b>	<b>Shelf Water Value (km/day)</b>
Mean	4.12	3.70
9th percentile	0.86	0.59
25th percentile	1.95	1.46
Median (50th percentile)	3.52	3.09
75th percentile	5.71	5.43
91st percentile	8.29	7.79
Standard Deviation	2.91	2.78

567

568

569 Table 3: Dates of weeks before, during and after Hurricane Alex for study consideration

<b>Storm Location</b>	<b>Dates Considered</b>
Before entering Gulf	6/19/2010 - 6/25/2010
Impacting Gulf	6/26/2010 - 7/2/2010
After exiting Gulf (Over land)	7/3/2010 - 7/9/2010

570

571

572 Table 4: Stokes drift magnitudes (km/day) of the weeks surrounding Hurricane Alex, in the area  
573 directly impacted by the storm.

<b>Parameter</b>	<b>Before Alex</b>	<b>During Alex</b>	<b>After Alex</b>
Mean	2.69	7.64	3.80
9th percentile	1.20	1.91	0.66
25th percentile	1.70	3.42	1.67
Median (50th percentile)	2.35	6.67	3.51
75th percentile	3.31	10.61	5.39
91st percentile	4.94	15.20	7.43
Standard Deviation	1.48	5.16	2.58

574

575

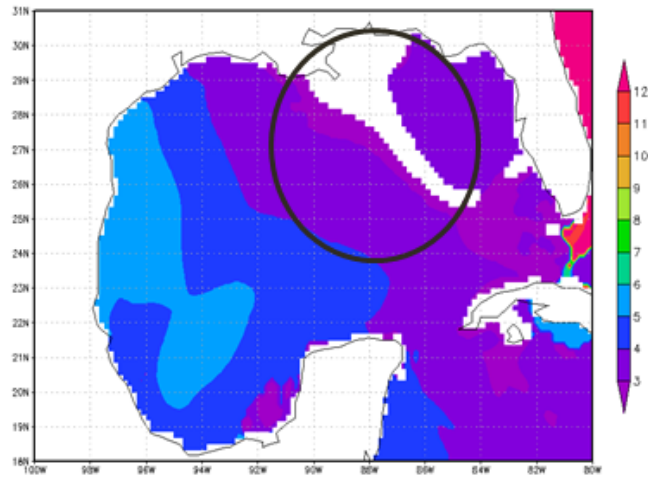
576 Table 5: Stokes drift magnitudes (km/day) of the weeks surrounding Hurricane Alex, in the area  
577 impacted by the oil spill.

<b>Parameter</b>	<b>Before Alex</b>	<b>During Alex</b>	<b>After Alex</b>
Mean	1.89	2.82	3.99
9th percentile	0.16	0.44	0.42
25th percentile	0.42	0.98	1.46
Median (50th percentile)	1.35	2.75	3.32
75th percentile	2.75	3.90	6.23
91st percentile	4.81	6.70	8.66
Standard Deviation	1.82	2.41	3.01

578

579

580 FIGURES:

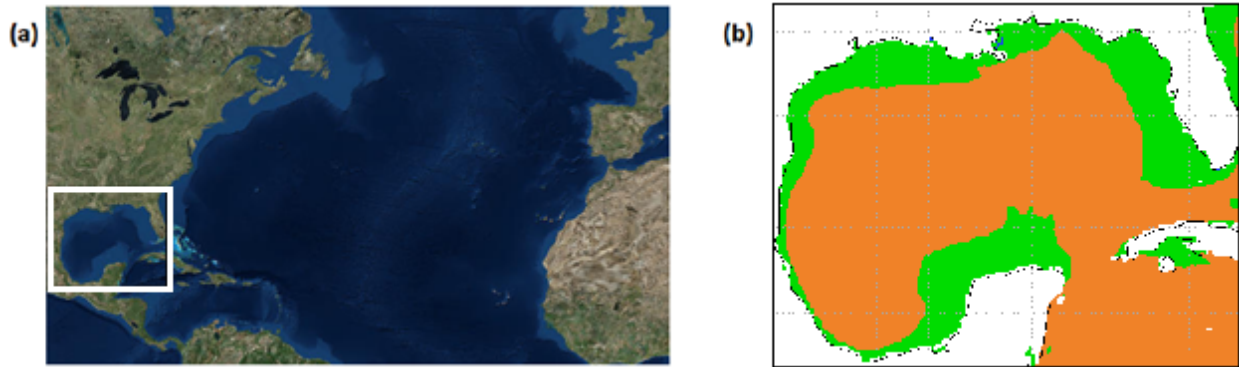


581

582 Figure 1: Example of NCEP peak wave period data (s), 1 May 2010 00Z. Problematic gap  
583 circled.

584

585

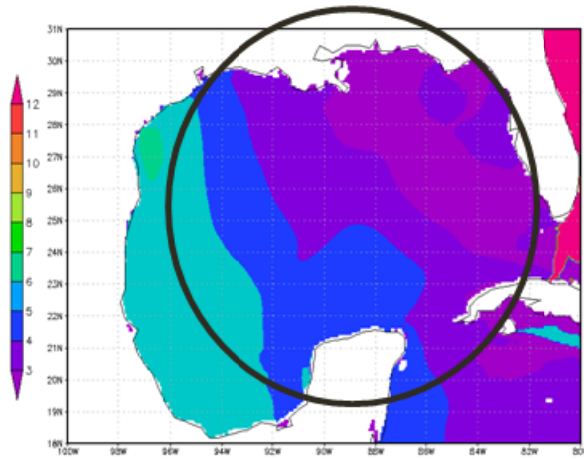


586

587 Figure 2: Maps showing extent of the model domains used for Wavewatch III. (a) 0.5° Atlantic  
588 Ocean grid with box indicating the location of the Gulf of Mexico grid. (b) 1/15° Gulf of  
589 Mexico grid with the green region indicating depths  $\leq 100$  m and the orange region  
590 indicating depths  $> 100$  m

591

592

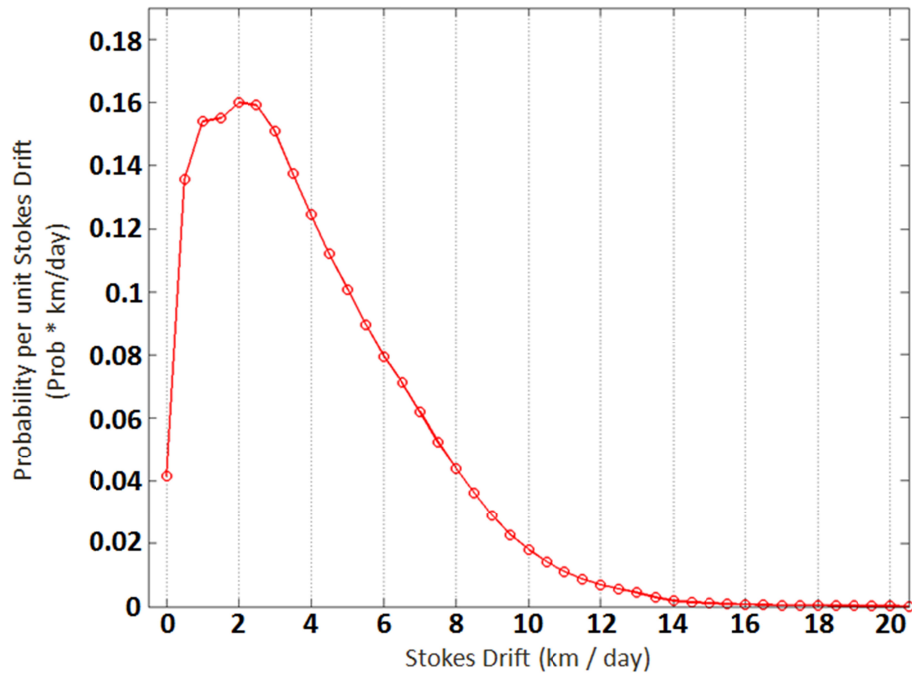


593

594 Figure 3: Example of WW3 modeled peak wave period data (s), 1 May 2010 00Z. The lack of a  
 595 gap in this data is circled.

596

597

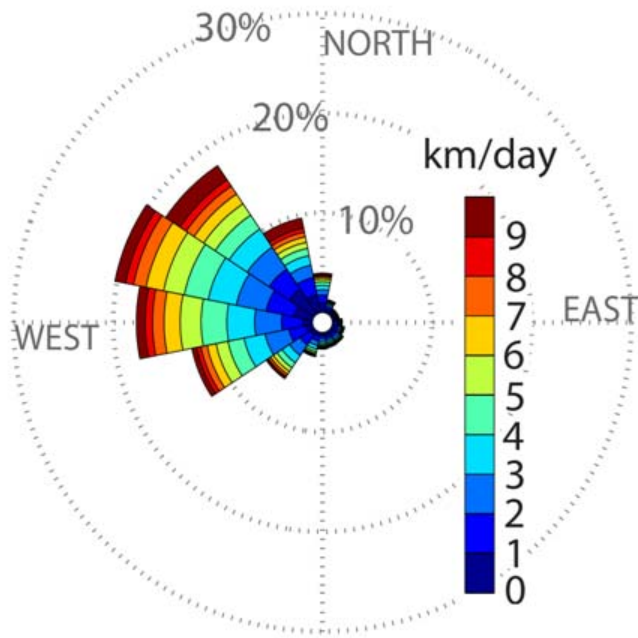


598

599 Figure 4: Probability density function of Stokes drift magnitude distributions in the Gulf of  
 600 Mexico, April-July 2010.

601

602

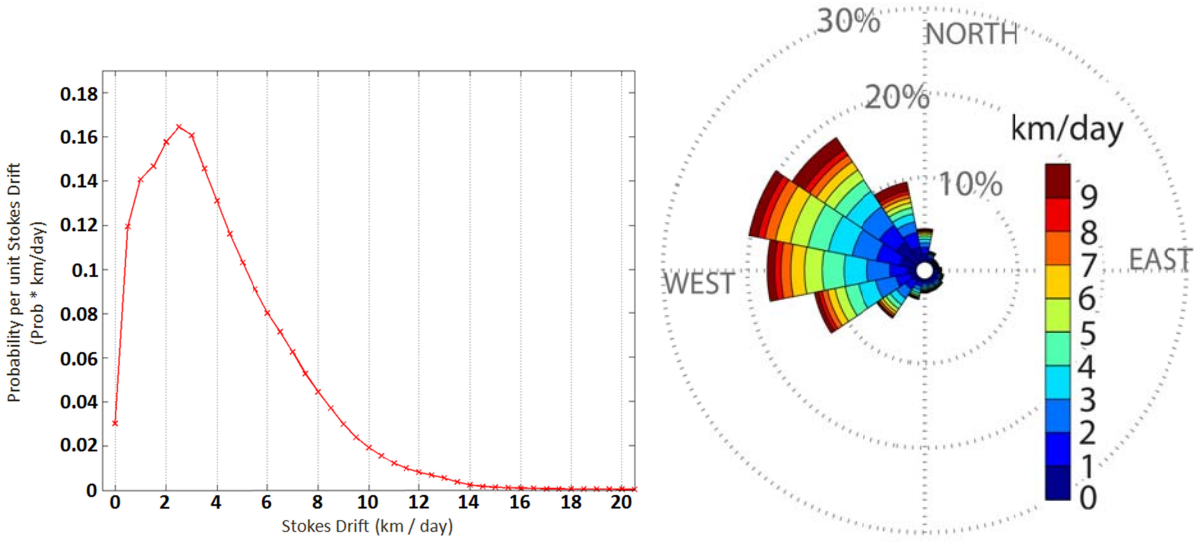


603

604 Figure 5: Directional rose plot of Stokes drift distributions in the Gulf of Mexico, April-July

605 2010. Directions are in oceanographic convention.

606



607

608

Figure 6: Probability distribution (left) and Directional rose plot (left) of Stokes drift

609

distributions in the Gulf of Mexico, April-July 2010, for water with depths >100m.

610

Directions are in oceanographic convention.

611

612

613

614

615

616

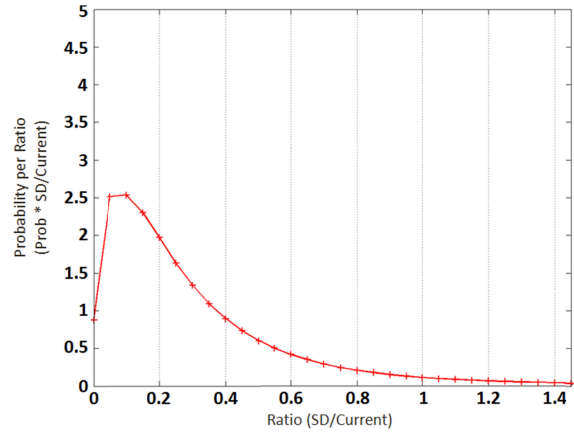
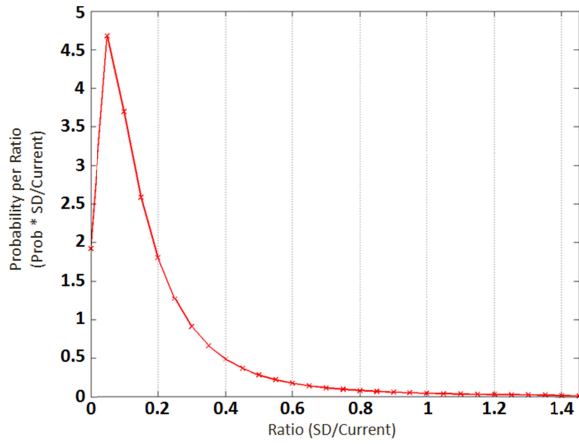
617

618

619

620

621



622

623 Figure 7: Probability density function of Stokes drift to surface current ratios in the Gulf  
 624 Mexico, from April-July 2010, for (left) waters deeper than 100 m, and (right) waters  
 625  $\leq 100$  m depth.

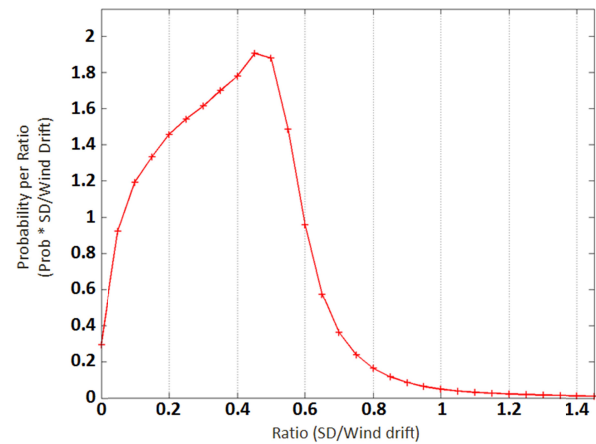
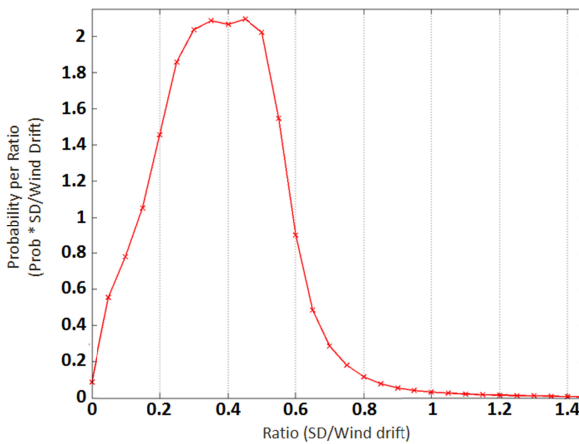
626

627

628

629

630



631

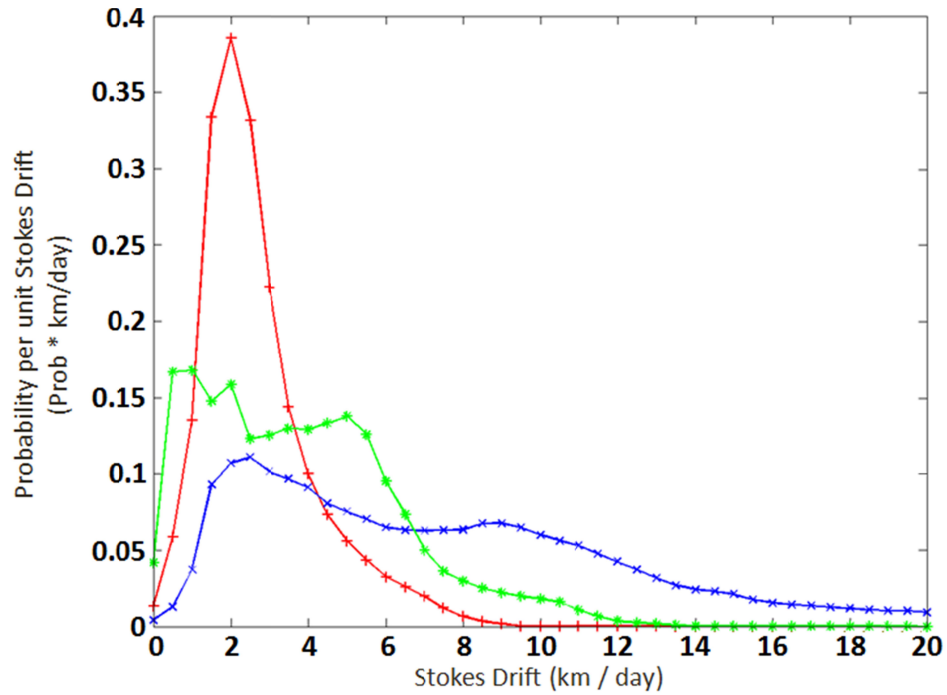
632 Figure 8: Probability density function of Stokes drift to wind drift ratios in the Gulf Mexico,  
633 April-July 2010 for (left) waters >100 m depth and (right) waters ≤100 m depth.. Wind  
634 drift is considered to be 2% of the 10 m wind speed.

635  
636  
637  
638  
639



640  
641 Figure 9: Map of Hurricane Alex storm track. Lower left box is area considered to be directly  
642 affected by storm. Upper right box is area considered to be affected by oil spill. From  
643 wunderground.com.

644  
645



646

647 Figure 10: Probability density functions of Stokes drift magnitudes in the area of the Gulf of

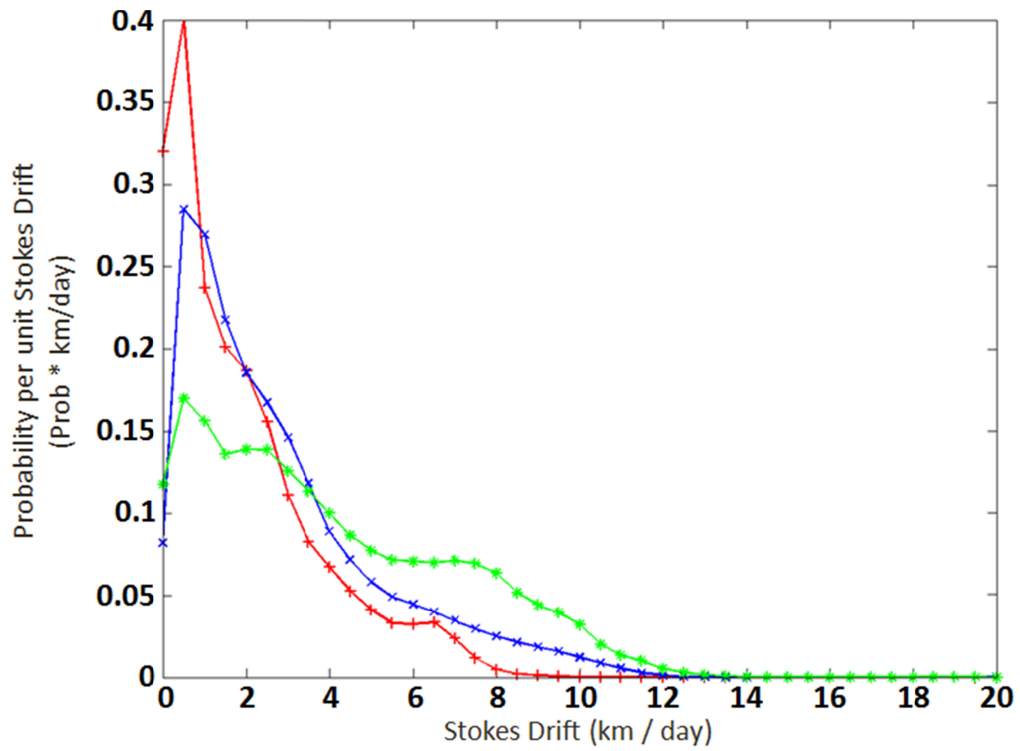
648 Mexico directly affected by Hurricane Alex. The red line with + marks is before the

649 storm; the blue line with x marks is during the storm, and the green line with \* marks is

650 after the storm.

651

652



653

654

Figure 11: Probability density functions of Stokes drift magnitudes in the area of the Gulf of

655

Mexico affected by the oil spill. The red line with + marks is before the storm; the blue

656

line with x marks is during the storm, and the green line with \* marks is after the storm.